Three-Dimensional Bulk Fermiology of $CeRu_2Ge_2$ in the Paramagnetic Phase by Soft X-Ray $h\nu$-Dependent (700–860 eV) ARPES

M. Yano,[1] A. Sekiyama,[1] H. Fujiwara,[1] T. Saita,[1] S. Imada,[1] T. Muro,[2] Y. Onuki,[3] and S. Suga[1]

[1]*Division of Materials Physics, Graduate School of Engineering Science, Osaka University, Toyonaka, Osaka 560-8531, Japan*

[2]*Japan Synchrotron Radiation Research Institute, SPring-8, Mikazuki, Hyogo 679-5198, Japan*

[3]*Department of Physics, Graduate School of Science, Osaka University, Toyonaka, Osaka 560-0043, Japan*

(Received 13 March 2006; published 18 January 2007)

By virtue of the soft x-ray angle-resolved photoelectron spectroscopy, the three-dimensional bulk fermiology has been successfully performed for a strongly correlated Ce compound, ferromagnet $CeRu_2Ge_2$ in the paramagnetic phase. A clear difference of the Fermi surface topology from either band calculation or de Haas–van Alphen results in the ferromagnetic phase is observed and interpreted by considering the difference of the $4f$ contribution to the Fermi surfaces in the paramagnetic phase.

DOI: 10.1103/PhysRevLett.98.036405 PACS numbers: 71.27.+a, 71.18.+y, 79.60.−i

Fermi surface (FS) topology dominates the macroscopic properties of solids such as resistivity, specific heat, and magnetic susceptibility. Therefore, the study of FSs is essential. The quantum oscillation measurement using the de Haas–van Alphen (dHvA) effect is known [1] as a powerful technique to evaluate the cross sections of the FSs. The dHvA measurement has so far been applied to many strongly correlated rare-earth materials [2–4]. The consistency between this experimentally observed FS and the band-structure calculation for $CeSn_3$ [5,6] is understood as the dHvA measurement, a conclusive tool to qualitatively judge whether the $4f$ electrons are ''itinerant'' or ''localized'' in the ground state of strongly correlated Ce compounds. However, a FS which is composed by high effective mass electrons could not be observed by the dHvA measurement [7] because the observation of such FSs requires a high-magnetic field and an ultralow temperature. In addition, the FSs change their shapes in accord with possible phase transitions at higher temperatures above several tens of K, where the dHvA measurement is inapplicable.

The low-$h\nu$ angle-resolved photoelectron spectroscopy (ARPES) is known to be a useful technique to reveal the characters of the two-dimensional and/or surface FSs as seen in many cases of high-T_C cuprates [8]. When the surface electronic structures are not much different from the bulk electronic structures, even surface-sensitive low-$h\nu$ ARPES with changing $h\nu$ in the normal emission could reveal the bulklike band dispersions along the surface normal direction [9]. As for correlated electron systems, however, the low-$h\nu$ three-dimensional (3D) ARPES band mapping has been rarely applied for fermiology except for the cases of simple transition metals [10] because the surface-vertical dispersion ($k_\perp$) is very different from the bulk $k_\perp$ dispersion. For rare-earth compounds, ARPES measurements have been performed for XRu_2Si_2 (X = La, Ce, Th, U) by using $h\nu$ within a range of 14–230 eV [11]. Recently, high-energy ($h\nu > 500$ eV) photoemission became feasible with high energy resolution and is found to be very effective for probing bulk electronic structures [12–15]. In this Letter, we demonstrate the potential of soft x-ray $h\nu$-dependent ARPES for clarifying the bulk 3D FS topology of a strongly correlated rare-earth compound, whose $4f$ electronic states are mutually very different between the bulk and the surface [13].

We have performed the 3D ARPES measurements for $CeRu_2Ge_2$ at 20 K which shows a ferromagnetic transition at $T_C \sim 8$ K [16,17]. $CeRu_2Ge_2$ crystallizes into a tetragonal $ThCr_2Si_2$-type structure with $a = 4.268$ Å and $c = 10.07$ Å (at 18 K [16]), whose Brillouin zone is shown in Fig. 1. The $4f$ electrons are thought to be rather localized and have a ferromagnetic alignment because of RKKY interaction under T_C [16,18,19]. On the other hand, isostructural $CeRu_2Si_2$ is a typical heavy fermion system which has itinerant $4f$ electrons [19,20]. The difference between these materials was observed by the bulk-sensitive $3d$-$4f$ resonant photoemission [13]. Thermoelectric power

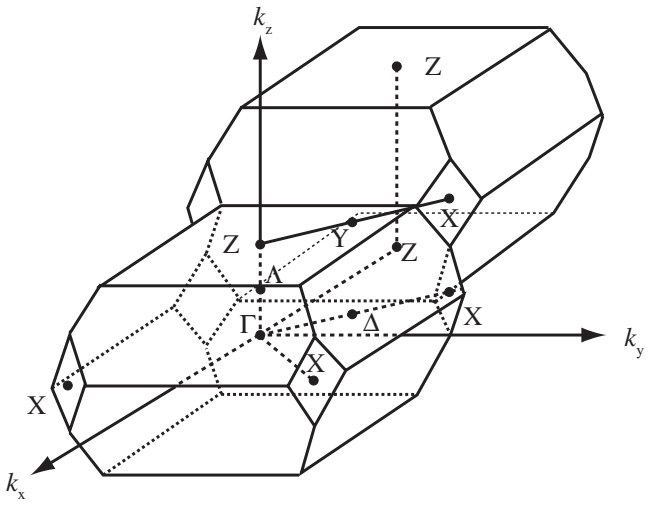

FIG. 1. Brillouin zone of the body-centered tetragonal crystal $CeRu_2Ge_2$ with $|\Gamma - \Lambda - Z| = 2\pi/c$, in plane $|\Gamma - Z| = 2\pi/a$.

has shown that the T_K of $CeRu_2Ge_2$ increases and the long-range magnetic ordering disappears under high pressures [21,22], suggesting that the electronic states under high pressures resemble those in $CeRu_2Si_2$. Thus, $CeRu_2Ge_2$ is a key material for discussing itinerancy and localization of Ce $4f$ electrons.

The $CeRu_2Ge_2$ single crystal was grown by the Czochralski pulling method. The high-energy ($h\nu =$ 700–860 eV) ARPES measurements have been performed with an energy step of 5 eV at BL25SU in SPring-8 [23]. The light incidence angle was ~45° with respect to the sample surface normal. The base pressure was about 3×10^{-8} Pa. We have performed the measurements at 20 K, where the sample is in the paramagnetic phase. The clean surface was obtained by cleaving *in situ* providing a (001) plane. A GAMMADATA-SCIENTA SES200 analyzer was used, covering more than a whole Brillouin zone along the direction of the slit. The energy resolution was set to ~200 meV for FS mappings. The angular resolution was ±0.1° and ±0.15° for the perpendicular and parallel direction to the analyzer slit, respectively. These values correspond to the momentum resolution of ±0.024 $Å^{-1}$ and ±0.035 $Å^{-1}$ at $h\nu = 700$ eV. The surface cleanliness was confirmed by the absence of the O $1s$ and C $1s$ photoemission signals. First, we have performed $k_z - k_{xy}$ mapping at several $h\nu$ and angles. In order to experimentally determine the exact value of $|k|$, we have taken the incident photon momentum into account [24]. After determining the $h\nu$ corresponding to the high symmetry points along the [001] direction, we have performed detailed angle-dependent ARPES for $k_x - k_y$ mapping. Then we have performed $h\nu$-dependent ARPES for $k_z - k_{xy}$ mapping through the high symmetry points in the k_{xy} Brillouin zone. We have alternated measurements of valence band and Ge $3d$ core spectra. Each valence band spectrum was normalized by the intensity of the Ge $3d$ spectra.

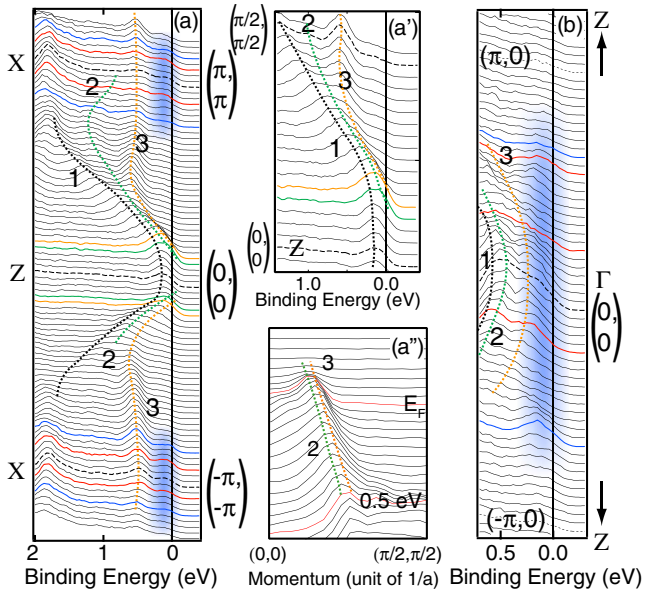

FIG. 2 (color online). ARPES spectra near E_F of $CeRu_2Ge_2$ with an energy resolution of ~200 meV. The dashed lines are guides to the eye. Each colored spectrum in EDCs corresponds to the Fermi wave number (k_F). (a) EDCs along the X-Z-X cut at $k_z \sim 2\pi/c$ ($h\nu = 755$ eV). (a′),(a″) Expanded EDCs and MDCs of (a) near the Z point, respectively. (b) EDCs near the Γ point along the Z-Γ-Z cut at $k_z \sim 0$ ($h\nu = 820$ eV). The shaded areas of (a) and (b) are located at bands 4 and 5 as discussed in text.

In order to analyze ARPES data as functions of binding energy and momentum, we have employed both energy distribution curves (EDCs) and momentum distribution curves (MDCs). Figures 2(a) and 2(b) show EDCs of $CeRu_2Ge_2$ along the in-plane X-Z-X direction and Z-Γ-Z direction, respectively. It is confirmed that five bands exist near the Fermi level (E_F) owing to the combination of both EDCs and MDCs. These bands are numbered from 1 to 5 from the lower binding energy. Figures 2(a′) and 2(a″) are the expanded EDCs and MDCs near the Z point along the X-Z-X direction, respectively. Bands 1, 2, and 3 are separately seen near the $(\pi/2, \pi/2)$ point, whereas bands 2 and 3 are almost overlapping around the Z point. Thus we interpret as the bands 2 and 3 cross E_F in Figs. 2(a′) and 2(a″). Furthermore, there are some structures corresponding to bands 4 and 5 above these three bands around the X point in Fig. 2(a) and the Γ point in Fig. 2(b) (shaded areas). The shapes of these bands will be discussed in detail in comparison with MDCs and the band calculation later.

We have integrated the intensities of MDCs in $E_F \pm 0.1$ eV as a function of momentum from a slice of ARPES data. The topology of the FSs thus obtained is displayed in Fig. 3. Figures 3(a) and 3(b) are $k_x - k_y$ maps at $k_z \sim 2\pi/c$ ($h\nu = 755$ eV) and $k_z \sim 0$ ($h\nu = 820$ eV), respectively. We have clearly observed the small holelike FS contours around the Z point derived from both bands 2 and 3 as shown in Fig. 3(a). Band 4 forms large holelike FSs centered at the Z point as obviously shown in both Figs. 3(a) and 3(b). Furthermore, we have recognized two Γ-concentric electronlike FSs and small FSs centered at the X point; these FSs are derived from band 5 [see MDCs of Figs. 5(b)–5(d)]. Figure 3(c) shows the slice of the FSs in the $k_z - k_{xy}$ plane [perpendicular to the plane of (a) and (b)] observed by $h\nu$-dependent ARPES. The FS contours of bands 2 and 3 have the shape of a vertically long ellipse centered at the Z point. The very large FS of band 4 compressed in the k_z direction can also be experimentally traced. Band 5 is confirmed to form continuous FSs along the ordinate X-X axis, although this FS is only partly observed near the Γ point resulting from the noticeable background from band 4.

From these three slices of the FSs, we have derived rough 3D shapes of the FSs as illustrated in Fig. 4. It is confirmed that $CeRu_2Ge_2$ in the paramagnetic phase has three types of FSs. The first and second types of the FSs correspond to an ellipsoidal shape centered at the Z point derived from bands 2 and 3 and a swelled-disk shape FS

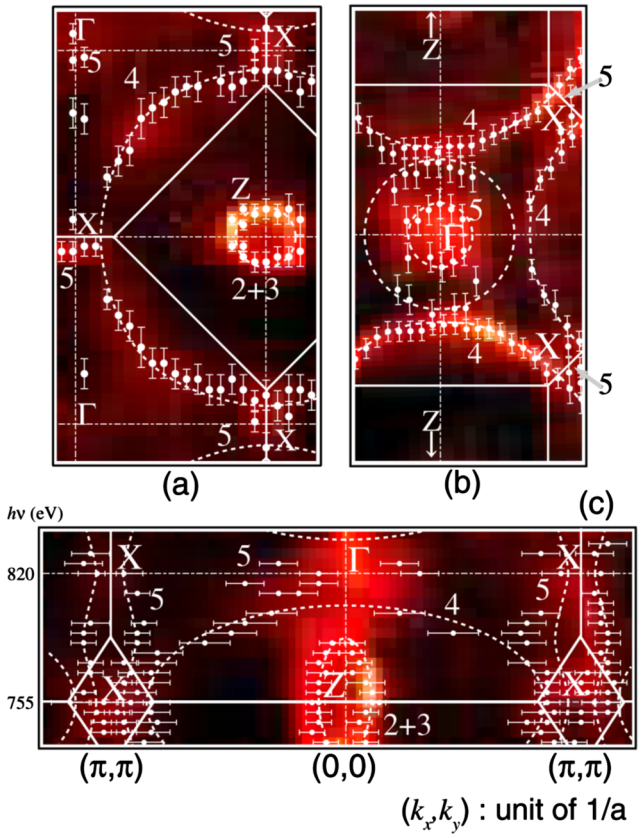

FIG. 3 (color online). FS slice of $CeRu_2Ge_2$ obtained by integrating the photoelectron intensity from +0.1 to −0.1 eV. The solid lines represent the corresponding Brillouin zone and the dash-dotted lines represent high symmetry lines. White dots (with error bars) represent the estimated k_F from EDCs and MDCs. The dashed lines represent the FSs following the experimentally evaluated k_F's. (a) FS slice at $k_z \sim 2\pi/c$ ($h\nu =$ 755 eV), (b) at $k_z \sim 0$ ($h\nu = 820$ eV). (c) FS slice in k_z (ordinate)—k_{xy} (abscissa) plane. Photon energies were varied from 735 to 840 eV with a 5 eV step. $h\nu = 820$ and 755 eV correspond to the Γ point and the Z points, respectively, along the Γ-Z direction.

invading into next Brillouin zones centered at the Z point from band 4 (left panel). The third one corresponds to a continuous rodlike shape FS along the X-X axis and a doughnutlike shape FS surrounding the Γ point from band 5 (right panel). More slices of the Brillouin zone are required for clarifying details of the FS shapes.

The observed ARPES data are compared with the augmented-plane-wave (APW) band calculation of paramagnetic $LaRu_2Ge_2$ [25] in Fig. 5(a), which corresponds to the Ce 4f electron localized model on the assumption that the 4f electrons in $CeRu_2Ge_2$ do not contribute to the construction of the dispersive bands. The band calculation predicts that there are three holelike FSs derived from bands 1–3 (corresponding to the ARPES results) and a large holelike FS derived from band 4, all of which are centered at the Z point. In addition, a doughnutlike electron pocket centered at the Γ point and a discontinuous FS along the ordinate X-X direction are predicted for band 5. This means that band 5 does not cross E_F near the X point in Fig. 5(a).

Five bands corresponding to bands 1 to 5 predicted for $LaRu_2Ge_2$ are clearly seen in Figs. 2 and 5(b)–5(d). However, the clear peak of band 1 located below E_F at about 0.14 eV at the Z point in Fig. 2(a′) is in a strong contrast to the prediction by the band-structure calculation for $LaRu_2Ge_2$, which predicts no quasiparticle peak below E_F at the Z point. Namely, band 1 is located on the occupied side and does not form a FS in our result. Furthermore, our experimental results show that band 5 exists on the occupied side at the X point forming a continuous FS. Figures 5(b) and 5(d) are the detailed MDCs near the X point $(\pi/a, \pi/a, 2\pi/c)$ at 755 eV and another X point $(\pi/a, \pi/a, 0)$ at 820 eV, respectively. These results confirm the continuity of the FS along the ordinate X-X direction as shown in Fig. 4.

In order to observe the FSs of $CeRu_2Ge_2$, the dHvA measurements in the ferromagnetic phase have been performed [26,27]. The dHvA measurement has confirmed all the predicted FS sheets spin-split corresponding to bands 1–5 calculated for $LaRu_2Ge_2$. Our ARPES results have, however, revealed that the FS derived from band 1 does not exist in the paramagnetic phase. It is also found that band 5 has a continuous FS along the k_z direction in this phase. These results are in a strong contrast to the dHvA results in the ferromagnetic phase. Although the FS of $CeRu_2Ge_2$ in the ferromagnetic phase is similar to that of $LaRu_2Ge_2$, the difference of our ARPES results from them are consistently understood if E_F of $CeRu_2Ge_2$ in the paramagnetic phase is energetically higher than that of the calculation for $LaRu_2Ge_2$. The E_F shift of $CeRu_2Ge_2$ in the paramagnetic phase from $LaRu_2Ge_2$ or $CeRu_2Ge_2$ in the ferromagnetic phase is thought to be due to the increased number of the electrons contributing to the near E_F bands in the paramagnetic $CeRu_2Ge_2$, where the weak but non-negligible hybridization of the Ce 4f electron should be additionally taken into account. The difference of the electric resistivity between $CeRu_2Ge_2$ and $LaRu_2Ge_2$ is suddenly diminished below T_C of $CeRu_2Ge_2$ [16], indicating the reduction of electron scattering due to the ferromagnetic ordering. This suggests that the contribution of

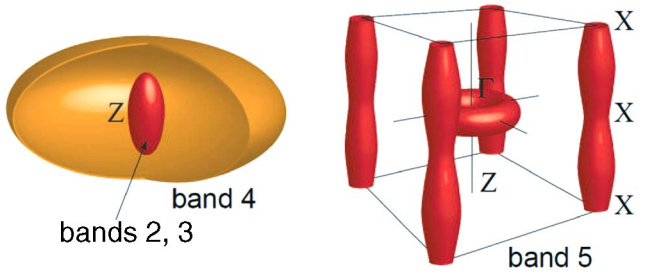

FIG. 4 (color online). The FS shape of each band imaged from Fig. 3. Left panel: Holelike FSs centered at the Z point derived from bands 2, 3, and 4. Right panel: Electron-like FS centered at the Γ point from band 5.

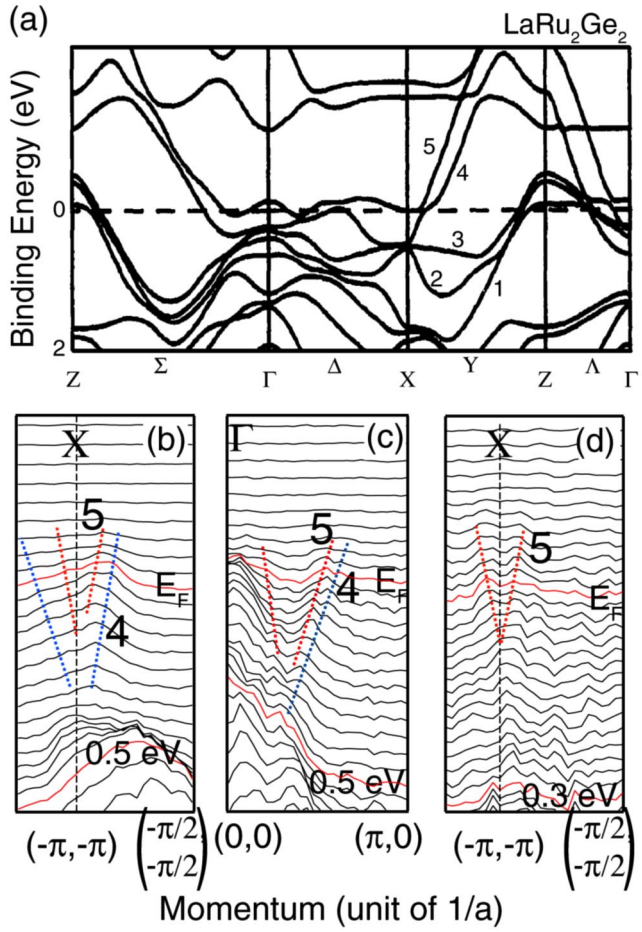

FIG. 5 (color online). (a) The band calculation with APW method for $LaRu_2Ge_2$ [25]. The FSs are formed by 5 bands. (b) MDCs displays of ARPES spectra near the X point along the X-Z direction at $k_z \sim 2\pi/c$ ($h\nu = 755$ eV). (c),(d) MDCs displays near the Γ point and the X point along the X-Γ direction at $k_z \sim 0$ ($h\nu = 820$ eV), respectively.

the $4f$ electrons to the FSs is reduced in the ferromagnetic phase due to the phase transition. Then the number of the electrons contributing to the FSs decreases below T_C. Accordingly, band 1 crosses E_F near the Z point and band 5 might form discontinuous FSs along the X-X (k_z) direction as predicted by the band-structure calculation.

We have performed 3D bulk-sensitive ARPES measurements for paramagnetic $CeRu_2Ge_2$ by using soft x rays. The detailed shapes of the FSs in the paramagnetic phase are revealed. The difference of the FS shapes from the dHvA results of ferromagnetic $CeRu_2Ge_2$ and the band calculation for $LaRu_2Ge_2$ is consistently understood by considering the Ce $4f$-conduction electron hybridization. It was found that the 3D ARPES will play an important role in the study of heavy fermion systems. Our results have clarified the contributions of $4f$ electrons in the strongly correlated system at high temperatures by the comparison between the ARPES result and the band calculation or the dHvA result.

We are grateful to H. Yamagami for fruitful discussions. We thank T. Miyamachi and H. Higashimichi for their help with the experiments. The present work was performed at SPring-8 under the proposal (2004A6009-NS-np, 2004B0400-NSa-np) supported by the Grant-in-Aids for Creative Scientific Research (15GS0213) of MEXT Japan and the 21st Century COE program (G18) of the Japan Society for the Promotion of Science.

[1] N. W. Ashcroft and N. D. Mermin, *Solid State Physics* (Saunders College, Philadelphia, 1976).
[2] H. Yamagami and A. Hasegawa, J. Phys. Soc. Jpn. **60**, 1011 (1991).
[3] P. H. P. Reinders, M. Springford, P. T. Coleridge, R. Boulet, and D. Ravot, Phys. Rev. Lett. **57**, 1631 (1986).
[4] G. Zwicknagl, Adv. Phys. **41**, 203 (1992).
[5] W. R. Johanson, G. W. Crabtree, A. S. Edelstein, and O. D. McMasters, Phys. Rev. Lett. **46**, 504 (1981).
[6] A. Hasegawa *et al.*, J. Phys. Soc. Jpn. **59**, 2457 (1990).
[7] H. Yamagami and A. Hasegawa, J. Phys. Soc. Jpn. **62**, 592 (1993).
[8] A. Damascelli, Z. Hussain, and Z.-X. Shen, Rev. Mod. Phys. **75**, 473 (2003).
[9] T.-C. Chiang, J. A. Knapp, M. Aono, and D. E. Eastman, Phys. Rev. B **21**, 3513 (1980).
[10] P. Aebi, T. J. Kreutz, J. Osterwalder, R. Fasel, P. Schwaller, and L. Schlapbach, Phys. Rev. Lett. **76**, 1150 (1996).
[11] J. D. Denlinger *et al.*, J. Electron Spectrosc. Relat. Phenom. **117**, 347 (2001).
[12] A. Sekiyama *et al.*, Nature (London) **403**, 396 (2000).
[13] A. Sekiyama *et al.*, J. Phys. Soc. Jpn. **69**, 2771 (2000).
[14] A. Sekiyama *et al.*, Phys. Rev. B **70**, 060506(R) (2004).
[15] S. Suga *et al.*, Phys. Rev. B **70**, 155106 (2004).
[16] M. J. Besnus *et al.*, Physica (Amsterdam) **171B**, 350 (1991).
[17] A. Böhm *et al.*, J. Magn. Magn. Mater. **76–77**, 150 (1988).
[18] A. Loidl *et al.*, Phys. Rev. B **46**, 9341 (1992).
[19] A. Loidl, G. Knopp, H. Spille, F. Steglich, and A. P. Murani, Physica (Amsterdam) **156B**, 794 (1989).
[20] G. G. Lonzarich, J. Magn. Magn. Mater. **76–77**, 1 (1988).
[21] H. Wilhelm, K. Alami-Yadri, B. Revaz, and D. Jaccard, Phys. Rev. B **59**, 3651 (1999).
[22] H. Wilhelm and D. Jaccard, Phys. Rev. B **69**, 214408 (2004).
[23] Y. Saitoh *et al.*, J. Synchrotron Radiat. **5**, 542 (1998).
[24] If an x ray was incident onto a sample at 45° with respect to the surface normal, for example, this incident photon has the momentum parallel ($q_\parallel$) and perpendicular ($q_\perp$) to the surface, which is $2\pi/\lambda(\text{Å})\sin 45° = 2\pi h\nu(\text{eV})/12\,398 \sin 45°$. When $h\nu = 700$ eV, the photon momentum values of both $|q_\parallel|$ and $|q_\perp|$ are about 0.25 Å^{-1}. Because the value $|k_z|$ of the first Brillouin zone of $CeRu_2Ge_2$ ($2\pi/c \sim 0.62$ Å^{-1}) is comparable to the value of the photon momentum, both $q_\parallel$ and $q_\perp$ cannot be negligible.
[25] H. Yamagami and A. Hasegawa, J. Phys. Soc. Jpn. **63**, 2290 (1994).
[26] C. A. King and G. G. Lonzarich, Physica (Amsterdam) **171B**, 161 (1991).
[27] H. Ikezawa *et al.*, Physica (Amsterdam) **237B**, 210 (1997).